EUROPEAN LABORATORY FOR PARTICLE PHYSICS

CERN-PPE/97-137
January 29, 1998

Search for the B_c Meson in Hadronic Z^0 Decays

The OPAL Collaboration

Abstract

A search for decays of the B_c meson was performed using data collected from 1990–1995 with the OPAL detector on or near the Z^0 peak at LEP. The decay channels $B_c^+ \to J/\psi\pi^+$, $B_c^+ \to J/\psi a_1^+$ and $B_c^+ \to J/\psi\ell^+\nu$ were investigated, where ℓ denotes an electron or a muon. Two candidates are observed in the mode $B_c^+ \to J/\psi\pi^+$, with an estimated background of (0.63 ± 0.20) events. The weighted mean of the masses of the two candidates is (6.32 ± 0.06) GeV/c^2, which is consistent with the predicted mass of the B_c meson. One candidate event is observed in the mode $B_c^+ \to J/\psi\ell^+\nu$, with an estimated background of (0.82 ± 0.19) events. No candidate events are observed in the $B_c^+ \to J/\psi a_1^+$ decay mode, with an estimated background of (1.10 ± 0.22) events. Upper bounds at the 90% confidence level are set on the production rates for these processes.

(Submitted to Physics Letters B)

The OPAL Collaboration

K. Ackerstaff[8], G. Alexander[23], J. Allison[16], N. Altekamp[5], K.J. Anderson[9], S. Anderson[12], S. Arcelli[2], S. Asai[24], S.F. Ashby[1], D. Axen[29], G. Azuelos[18,a], A.H. Ball[17], E. Barberio[8], R.J. Barlow[16], R. Bartoldus[3], J.R. Batley[5], S. Baumann[3], J. Bechtluft[14], C. Beeston[16], T. Behnke[8], A.N. Bell[1], K.W. Bell[20], G. Bella[23], S. Bentvelsen[8], S. Bethke[14], S. Betts[15], O. Biebel[14], A. Biguzzi[5], S.D. Bird[16], V. Blobel[27], I.J. Bloodworth[1], J.E. Bloomer[1], M. Bobinski[10], P. Bock[11], D. Bonacorsi[2], M. Boutemeur[34], S. Braibant[8], L. Brigliadori[2], R.M. Brown[20], H.J. Burckhart[8], C. Burgard[8], R. Bürgin[10], P. Capiluppi[2], R.K. Carnegie[6], A.A. Carter[13], J.R. Carter[5], C.Y. Chang[17], D.G. Charlton[1,b], D. Chrisman[4], P.E.L. Clarke[15], I. Cohen[23], J.E. Conboy[15], O.C. Cooke[8], C. Couyoumtzelis[13], R.L. Coxe[9], M. Cuffiani[2], S. Dado[22], C. Dallapiccola[17], G.M. Dallavalle[2], R. Davis[30], S. De Jong[12], L.A. del Pozo[4], K. Desch[3], B. Dienes[33,d], M.S. Dixit[7], M. Doucet[18], E. Duchovni[26], G. Duckeck[34], I.P. Duerdoth[16], D. Eatough[16], J.E.G. Edwards[16], P.G. Estabrooks[6], H.G. Evans[9], M. Evans[13], F. Fabbri[2], A. Fanfani[2], M. Fanti[2], A.A. Faust[30], L. Feld[8], F. Fiedler[27], M. Fierro[2], H.M. Fischer[3], I. Fleck[8], R. Folman[26], D.G. Fong[17], M. Foucher[17], A. Fürtjes[8], D.I. Futyan[16], P. Gagnon[7], J.W. Gary[4], J. Gascon[18], S.M. Gascon-Shotkin[17], N.I. Geddes[20], C. Geich-Gimbel[3], T. Geralis[20], G. Giacomelli[2], P. Giacomelli[4], R. Giacomelli[2], V. Gibson[5], W.R. Gibson[13], D.M. Gingrich[30,a], D. Glenzinski[9], J. Goldberg[22], M.J. Goodrick[5], W. Gorn[4], C. Grandi[2], E. Gross[26], J. Grunhaus[23], M. Gruwé[8], C. Hajdu[32], G.G. Hanson[12], M. Hansroul[8], M. Hapke[13], C.K. Hargrove[7], P.A. Hart[9], C. Hartmann[3], M. Hauschild[8], C.M. Hawkes[5], R. Hawkings[27], R.J. Hemingway[6], M. Herndon[17], G. Herten[10], R.D. Heuer[8], M.D. Hildreth[8], J.C. Hill[5], S.J. Hillier[1], P.R. Hobson[25], A. Hocker[9], R.J. Homer[1], A.K. Honma[28,a], D. Horváth[32,c], K.R. Hossain[30], R. Howard[29], P. Hüntemeyer[27], D.E. Hutchcroft[5], P. Igo-Kemenes[11], D.C. Imrie[25], M.R. Ingram[16], K. Ishii[24], A. Jawahery[17], P.W. Jeffreys[20], H. Jeremie[18], M. Jimack[1], A. Joly[18], C.R. Jones[5], G. Jones[16], M. Jones[6], U. Jost[11], P. Jovanovic[1], T.R. Junk[8], J. Kanzaki[24], D. Karlen[6], V. Kartvelishvili[16], K. Kawagoe[24], T. Kawamoto[24], P.I. Kayal[30], R.K. Keeler[28], R.G. Kellogg[17], B.W. Kennedy[20], J. Kirk[29], A. Klier[26], S. Kluth[8], T. Kobayashi[24], M. Kobel[10], D.S. Koetke[6], T.P. Kokott[3], M. Kolrep[10], S. Komamiya[24], T. Kress[11], P. Krieger[6], J. von Krogh[11], P. Kyberd[13], G.D. Lafferty[16], R. Lahmann[17], W.P. Lai[19], D. Lanske[14], J. Lauber[15], S.R. Lautenschlager[31], J.G. Layter[4], D. Lazic[22], A.M. Lee[31], E. Lefebvre[18], D. Lellouch[26], J. Letts[12], L. Levinson[26], S.L. Lloyd[13], F.K. Loebinger[16], G.D. Long[28], M.J. Losty[7], J. Ludwig[10], D. Lui[12], A. Macchiolo[2], A. Macpherson[30], M. Mannelli[8], S. Marcellini[2], C. Markopoulos[13], C. Markus[3], A.J. Martin[13], J.P. Martin[18], G. Martinez[17], T. Mashimo[24], P. Mättig[3], W.J. McDonald[30], J. McKenna[29], E.A. Mckigney[15], T.J. McMahon[1], R.A. McPherson[8], F. Meijers[8], S. Menke[3], F.S. Merritt[9], H. Mes[7], J. Meyer[27], A. Michelini[2], G. Mikenberg[26], D.J. Miller[15], A. Mincer[22,e], R. Mir[26], W. Mohr[10], A. Montanari[2], T. Mori[24], U. Müller[3], S. Mihara[24], K. Nagai[26], I. Nakamura[24], H.A. Neal[8], B. Nellen[3], R. Nisius[8], S.W. O'Neale[1], F.G. Oakham[7], F. Odorici[2], H.O. Ogren[12], A. Oh[27], N.J. Oldershaw[16], M.J. Oreglia[9], S. Orito[24], J. Pálinkás[33,d], G. Pásztor[32], J.R. Pater[16], G.N. Patrick[20], J. Patt[10], R. Perez-Ochoa[8], S. Petzold[27], P. Pfeifenschneider[14], J.E. Pilcher[9], J. Pinfold[30], D.E. Plane[8], P. Poffenberger[28], B. Poli[2], A. Posthaus[3], C. Rembser[8], S. Robertson[28], S.A. Robins[22], N. Rodning[30], J.M. Roney[28], A. Rooke[15], A.M. Rossi[2], P. Routenburg[30], Y. Rozen[22], K. Runge[10], O. Runolfsson[8], U. Ruppel[14], D.R. Rust[12], R. Rylko[25], K. Sachs[10], T. Saeki[24], W.M. Sang[25], E.K.G. Sarkisyan[23], C. Sbarra[29], A.D. Schaile[34], O. Schaile[34], F. Scharf[3], P. Scharff-Hansen[8], J. Schieck[11], P. Schleper[11], B. Schmitt[8], S. Schmitt[11], A. Schöning[8], M. Schröder[8], H.C. Schultz-Coulon[10], M. Schumacher[3], C. Schwick[8], W.G. Scott[20], T.G. Shears[16], B.C. Shen[4], C.H. Shepherd-Themistocleous[8], P. Sherwood[15], G.P. Siroli[2], A. Sittler[27], A. Skillman[15], A. Skuja[17], A.M. Smith[8], G.A. Snow[17], R. Sobie[28], S. Söldner-Rembold[10], R.W. Springer[30], M. Sproston[20], K. Stephens[16], J. Steuerer[27], B. Stockhausen[3], K. Stoll[10], D. Strom[19], R. Ströhmer[34], P. Szymanski[20], R. Tafirout[18], S.D. Talbot[1], S. Tanaka[24], P. Taras[18], S. Tarem[22], R. Teuscher[8], M. Thiergen[10], M.A. Thomson[8], E. von Törne[3],

E. Torrence[8], S. Towers[6], I. Trigger[18], Z. Trócsányi[33], E. Tsur[23], A.S. Turcot[9], M.F. Turner-Watson[8], P. Utzat[11], R. Van Kooten[12], M. Verzocchi[10], P. Vikas[18], E.H. Vokurka[16], H. Voss[3], F. Wäckerle[10], A. Wagner[27], C.P. Ward[5], D.R. Ward[5], P.M. Watkins[1], A.T. Watson[1], N.K. Watson[1], P.S. Wells[8], N. Wermes[3], J.S. White[28], B. Wilkens[10], G.W. Wilson[27], J.A. Wilson[1], T.R. Wyatt[16], S. Yamashita[24], G. Yekutieli[26], V. Zacek[18], D. Zer-Zion[8]

[1]School of Physics and Space Research, University of Birmingham, Birmingham B15 2TT, UK
[2]Dipartimento di Fisica dell' Università di Bologna and INFN, I-40126 Bologna, Italy
[3]Physikalisches Institut, Universität Bonn, D-53115 Bonn, Germany
[4]Department of Physics, University of California, Riverside CA 92521, USA
[5]Cavendish Laboratory, Cambridge CB3 0HE, UK
[6] Ottawa-Carleton Institute for Physics, Department of Physics, Carleton University, Ottawa, Ontario K1S 5B6, Canada
[7]Centre for Research in Particle Physics, Carleton University, Ottawa, Ontario K1S 5B6, Canada
[8]CERN, European Organisation for Particle Physics, CH-1211 Geneva 23, Switzerland
[9]Enrico Fermi Institute and Department of Physics, University of Chicago, Chicago IL 60637, USA
[10]Fakultät für Physik, Albert Ludwigs Universität, D-79104 Freiburg, Germany
[11]Physikalisches Institut, Universität Heidelberg, D-69120 Heidelberg, Germany
[12]Indiana University, Department of Physics, Swain Hall West 117, Bloomington IN 47405, USA
[13]Queen Mary and Westfield College, University of London, London E1 4NS, UK
[14]Technische Hochschule Aachen, III Physikalisches Institut, Sommerfeldstrasse 26-28, D-52056 Aachen, Germany
[15]University College London, London WC1E 6BT, UK
[16]Department of Physics, Schuster Laboratory, The University, Manchester M13 9PL, UK
[17]Department of Physics, University of Maryland, College Park, MD 20742, USA
[18]Laboratoire de Physique Nucléaire, Université de Montréal, Montréal, Quebec H3C 3J7, Canada
[19]University of Oregon, Department of Physics, Eugene OR 97403, USA
[20]Rutherford Appleton Laboratory, Chilton, Didcot, Oxfordshire OX11 0QX, UK
[22]Department of Physics, Technion-Israel Institute of Technology, Haifa 32000, Israel
[23]Department of Physics and Astronomy, Tel Aviv University, Tel Aviv 69978, Israel
[24]International Centre for Elementary Particle Physics and Department of Physics, University of Tokyo, Tokyo 113, and Kobe University, Kobe 657, Japan
[25]Brunel University, Uxbridge, Middlesex UB8 3PH, UK
[26]Particle Physics Department, Weizmann Institute of Science, Rehovot 76100, Israel
[27]Universität Hamburg/DESY, II Institut für Experimental Physik, Notkestrasse 85, D-22607 Hamburg, Germany
[28]University of Victoria, Department of Physics, P O Box 3055, Victoria BC V8W 3P6, Canada
[29]University of British Columbia, Department of Physics, Vancouver BC V6T 1Z1, Canada
[30]University of Alberta, Department of Physics, Edmonton AB T6G 2J1, Canada
[31]Duke University, Dept of Physics, Durham, NC 27708-0305, USA
[32]Research Institute for Particle and Nuclear Physics, H-1525 Budapest, P O Box 49, Hungary
[33]Institute of Nuclear Research, H-4001 Debrecen, P O Box 51, Hungary
[34]Ludwigs-Maximilians-Universität München, Sektion Physik, Am Coulombwall 1, D-85748 Garching, Germany

[a] and at TRIUMF, Vancouver, Canada V6T 2A3
[b] and Royal Society University Research Fellow
[c] and Institute of Nuclear Research, Debrecen, Hungary
[d] and Department of Experimental Physics, Lajos Kossuth University, Debrecen, Hungary
[e] and Department of Physics, New York University, NY 1003, USA

1 Introduction

The ground-state pseudoscalar mesons containing a b quark have all been observed, by experiments at CESR, DORIS, LEP and the TEVATRON, except for the beauty-charm meson $B_c(\bar{b}c)$. The B_c meson can be produced at LEP in hadronic Z^0 decays. Using the non-relativistic potential model for heavy quark bound states, the mass of the B_c meson is predicted to be in the range 6.24 to 6.31 GeV/c^2 [1]. The production mechanism for the $\bar{b}c$ bound states differs from that of the B_d, B_u and B_s mesons, since the soft fragmentation process, involving spontaneous creation of $b\bar{b}$ or $c\bar{c}$, is severely suppressed. The predicted dominant production mechanism shown in figure 1 involves the emission and splitting to $c\bar{c}$ of a hard gluon in the process $Z^0 \to b\bar{b}$ [2]. Perturbative QCD calculations predict a production rate of 10^{-5} to 10^{-4} B_c per hadronic Z^0 decay, with a momentum spectrum that is considerably softer than that of the lighter B hadrons [3] (see figure 2). The decay of the B_c meson is governed by the weak interaction; strong decay into a lower mass beauty meson and a charmed hadron is forbidden by energy conservation. There is a large spread in the predictions for the B_c lifetime, although it is generally agreed that it is shorter than the lifetime of the light B mesons. Theoretical calculations predict a significant branching ratio into modes involving the J/ψ meson [4].

In this article we report on a search for B_c decays in a data sample of 4.2×10^6 hadronic Z^0 decays collected with the OPAL detector at LEP. A previous article by the OPAL collaboration [5] reported on a study of J/ψ meson production in hadronic Z^0 decays, and the reconstruction of exclusive decays of B hadrons into modes containing a J/ψ meson. This analysis included a candidate for the decay [1] $B_c^+ \to J/\psi\pi^+$. The analysis of the B_c decays is extended to include searches for the decay modes $B_c^+ \to J/\psi a_1^+$ and $B_c^+ \to J/\psi\ell^+\nu$, as well as $B_c^+ \to J/\psi\pi^+$, where ℓ denotes an electron or a muon.

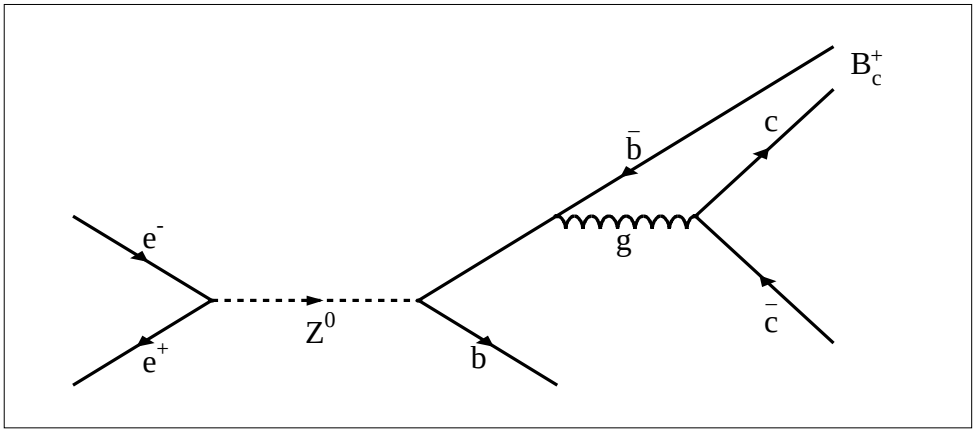

Figure 1: Feynman Diagram for the predicted production process $Z^0 \to b\bar{b} \to B_cX$

2 The OPAL Detector

The OPAL detector is described in detail elsewhere [6]. Here we briefly describe the components which are relevant to this analysis. The OPAL coordinate system is defined with the z-axis following the electron beam direction, the x-axis pointing towards the center of the LEP ring and the y-axis pointing upwards, forming a right-handed coordinate system. The polar angle θ is defined relative to the z-axis, and r and ϕ are the standard cylindrical polar coordinates. Charged particle tracking is

[1] Throughout this article charge conjugate modes are implied.

performed by the central detector system that is located in a solenoidal magnetic field of 0.435 T. The central tracking system consists of a two layer silicon microvertex detector, installed before the 1991 run [7], a high precision vertex drift chamber, a large volume jet chamber and a set of planar drift z-chambers measuring track coordinates along z. The momentum resolution of the central detector in the x-y plane is $(\delta p_{xy}/p_{xy})^2 = (2\%)^2 + (0.15\% \cdot p_{xy})^2$, where p_{xy} is in GeV/c. Particle identification is provided by the measurement of specific ionization, $\mathrm{d}E/\mathrm{d}x$, in the jet chamber. The $\mathrm{d}E/\mathrm{d}x$ resolution for tracks with the maximum of 159 samplings in the jet chamber is 3.5% [8]. The central detector is surrounded by a lead glass electromagnetic calorimeter with a pre-sampler. The magnet yoke is instrumented with layers of streamer tubes that serve as a hadron calorimeter and provide additional information for muon identification. Four layers of planar drift chambers surrounding the detector provide tracking for muons.

3 Data Sample and Event Selection

The data used in this study were collected between 1990 and 1995 using the OPAL detector at LEP. The sample corresponds to approximately 4.2×10^6 hadronic Z^0 decays. The selection of hadronic events has been described elsewhere [9]. The selection efficiency for the multihadronic events is $(98.1 \pm 0.5)\%$, with a background of less than 0.1%.

For this analysis we impose the following additional requirements on charged tracks: the number of hits in the central detector used for the reconstruction of a track must be greater than 40 (this restricts the acceptance to $|\cos\theta| < 0.94$); the distance of closest approach to the beam axis in the x-y plane must be less than 0.5 cm; the transverse momentum with respect to the beam direction must exceed 0.25 GeV/c; and the total momentum of the track must exceed 0.5 GeV/c. To obtain accurate polar angle measurements, a barrel ($|\cos\theta| < 0.72$) track is required to match with a z-chamber track segment containing at least 3 hits; forward going tracks are constrained to the point where they leave the chamber.

A track is identified as a pion if the $\mathrm{d}E/\mathrm{d}x$ probability for the pion hypothesis, that is the probability that the specific ionization energy loss in the jet chamber ($\mathrm{d}E/\mathrm{d}x$) is compatible with that expected for a pion, exceeds 2.5% if the measured $\mathrm{d}E/\mathrm{d}x$ is lower than the expected $\mathrm{d}E/\mathrm{d}x$ for a pion, and 0.1% if it is higher. For the purpose of background rejection, tracks are identified as kaons if the $\mathrm{d}E/\mathrm{d}x$ probability for the kaon hypothesis is greater than 5%.

Leptons are identified by imposing the following selection criteria. We require the track momentum $p > 2.0$ GeV/c, and $|\cos\theta| < 0.9$. For electron identification we use a neural network algorithm [10] which uses twelve variables containing information from the central tracking system, the electromagnetic calorimeter and its pre-sampler. The overall efficiency for the identification of electrons from B hadron decays is $(77 \pm 5)\%$. The error in the electron identification efficiency was determined by comparing the efficiencies in Monte Carlo and data for a pure sample of electrons from photon conversions. For muon identification, two sets of selection criteria are used. For muon candidates combined to form J/ψ candidates in the $\mathrm{B}_\mathrm{c}^+ \to \mathrm{J}/\psi\pi^+$ and $\mathrm{B}_\mathrm{c}^+ \to \mathrm{J}/\psi\mathrm{a}_1^+$ modes we employ a "normal" muon selection. In this selection we require a ϕ-θ match between the extrapolated muon candidate track and a track segment reconstructed in the muon chamber [11]. In addition, we require that the candidate muon track be the best match to the muon segment. When no match to a muon segment is found, we search for a match with a track segment in the hadron calorimeter [12]. The efficiency for this "normal" muon identification is $(85 \pm 4)\%$. The errors for the muon identification were determined by comparing the efficiency between Monte Carlo and data for a pure sample of muons from muon pair events. For any muon candidates combined to form $\mathrm{B_c}$ candidates in the decay $\mathrm{B}_\mathrm{c}^+ \to \mathrm{J}/\psi\ell^+\nu$, where $\mathrm{J}/\psi \to \ell^+\ell^-$, we employ a "strong" muon identification [13]. In this selection we use only tracks matched with track segments in the muon detector, reject tracks identified as kaons using $\mathrm{d}E/\mathrm{d}x$ information, and apply an isolation cut by requiring that there be less than 20 track segments in the muon detector within 0.3 radians of the track. The efficiency for this "strong" muon identification used in the $\mathrm{B_c} \to \mathrm{J}/\psi\ell\nu$

mode is (76 $\pm$ 4)%.

Events are organised into jets of particles which are constructed using charged tracks and neutral clusters that are not associated to any charged track [14]. To form jets we use the scaled invariant mass jet-finding algorithm of JADE with a jet resolution parameter $y_{\rm cut} = 0.04$.

A Monte Carlo simulation is used to determine the reconstruction and selection efficiencies for the various decay modes and for estimating the background level. The process $\mathrm{Z^0 \to b\bar{b} \to B_c X}$ (figure 1) and subsequent $\mathrm{B_c}$ meson decays are simulated using the JETSET 7.4 program [15]. Figure 2 shows the prediction of reference [2] for the $\mathrm{B_c}$ momentum spectrum along with the JETSET 7.4 simulation of the $\mathrm{B_c}$ spectrum. In addition to simulating $\mathrm{B_c}$ production as described in reference [2], JETSET 7.4 includes contributions from the production of excited states of $\mathrm{\bar{b}c}$ bound states. The two momentum distributions are similar. Also shown is the distribution for light b hadrons given by the Peterson et al. fragmentation function [16] with its parameter tuned to produce the measured mean energy fraction ($\langle x_E \rangle = E_{\rm B}/E_{\rm beam}$), indicating that the $\mathrm{B_c}$ spectrum is predicted to be considerably softer than that for the light b hadrons. The measured mean energy fraction ($\langle x_E \rangle$) for the light b hadrons is $\langle x_E \rangle = 0.695 \pm 0.006 \pm 0.008$ [17], while for the generated $\mathrm{B_c}$ meson we find $\langle x_E \rangle = 0.54$. Samples of 2000 events were simulated for each of the following decay modes: $\mathrm{B_c^+ \to J/\psi \pi^+}$, $\mathrm{B_c^+ \to J/\psi a_1^+}$, where $\mathrm{a_1^+ \to \rho^0 \pi^+}$ and $\rho^0 \to \pi^+\pi^-$, and the semileptonic mode $\mathrm{B_c^+ \to J/\psi \ell^+ \nu}$, where ℓ denotes an electron or a muon. In each event the $\mathrm{J/\psi}$ decays to $\ell^+\ell^-$.

A simulated event sample of 4×10^6 five-flavor hadronic $\mathrm{Z^0}$ decays, nearly equal in size to the data sample, was used for studying the background processes. A sample of 80,000 hadronic $\mathrm{Z^0}$ decays containing the process $\mathrm{B \to J/\psi X}$, where a $\mathrm{J/\psi \to \ell^+\ell^-}$ decay is present in each event, was used to increase the statistical significance of the background study. In addition two samples of 4000 events containing the processes $\mathrm{Z^0 \to J/\psi q\bar{q}}$ and $\mathrm{Z^0 \to J/\psi c\bar{c}}$ were produced in order to study background due to prompt $\mathrm{J/\psi}$ production from gluon fragmentation and c quark fragmentation, respectively. The JETSET 7.4 parton shower Monte Carlo generator is used for the simulation of the hadronic $\mathrm{Z^0}$ decays. For the fragmentation of heavy quarks into charmed and light b-flavored hadrons, we use the Peterson fragmentation function. JETSET 7.4 parameters and branching ratios were tuned to match experimental results [18] [19]. All simulated events are passed through the full simulation of the OPAL detector [20]. JETSET does not include radiative decay of $\mathrm{J/\psi}$ into lepton pairs. The presence of unreconstructed final state radiation (FSR) in the decay $\mathrm{J/\psi \to \ell^+\ell^-\gamma}$ produces a tail toward lower masses in the invariant mass distribution. The effect of FSR on the $\mathrm{J/\psi}$ mass distribution is included in Monte Carlo events at reconstruction level. The photon energy is calculated using first order perturbative QED [21]. An error is calculated to account for the higher order terms [22]. Excepting the FSR correction for Monte Carlo simulated events, data and Monte Carlo simulated samples are analysed using the same reconstruction program.

4 Search for $\mathrm{B_c}$ decays

We search for the decay modes $\mathrm{B_c^+ \to J/\psi \pi^+}$, $\mathrm{B_c^+ \to J/\psi a_1^+}$, where $\mathrm{a_1^+ \to \rho^0 \pi^+}$ and $\rho^0 \to \pi^+\pi^-$, and the semileptonic mode $\mathrm{B_c^+ \to J/\psi \ell^+ \nu}$. The analysis involves the reconstruction of $\mathrm{J/\psi}$ candidates in the leptonic mode $\mathrm{J/\psi \to \ell^+\ell^-}$, which are then combined with other tracks to form $\mathrm{J/\psi \pi^+}$, $\mathrm{J/\psi \pi^+\pi^-\pi^+}$, and $\mathrm{J/\psi \ell^+}$ combinations. The $\mathrm{J/\psi \ell^+}$ combination is a partial reconstruction of the mode $\mathrm{B_c^+ \to J/\psi \ell^+ \nu}$. Candidates are formed from charged tracks which are assigned to the same jet.

4.1 Reconstruction of $\mathrm{J/\psi}$ Decays

The $\mathrm{J/\psi}$ meson decays are reconstructed in the leptonic modes $\mathrm{J/\psi \to \mu^+\mu^-}$ and $\mathrm{J/\psi \to e^+e^-}$. A pair of opposite sign electron or muon candidates in the same jet, with an invariant mass consistent with the $\mathrm{J/\psi}$ mass, is considered a $\mathrm{J/\psi}$ candidate. Muon candidates combined to form $\mathrm{J/\psi}$ candidates in the $\mathrm{B_c^+ \to J/\psi \pi^+}$ and $\mathrm{B_c^+ \to J/\psi a_1^+}$ modes must satisfy the "normal" muon identification. Muon

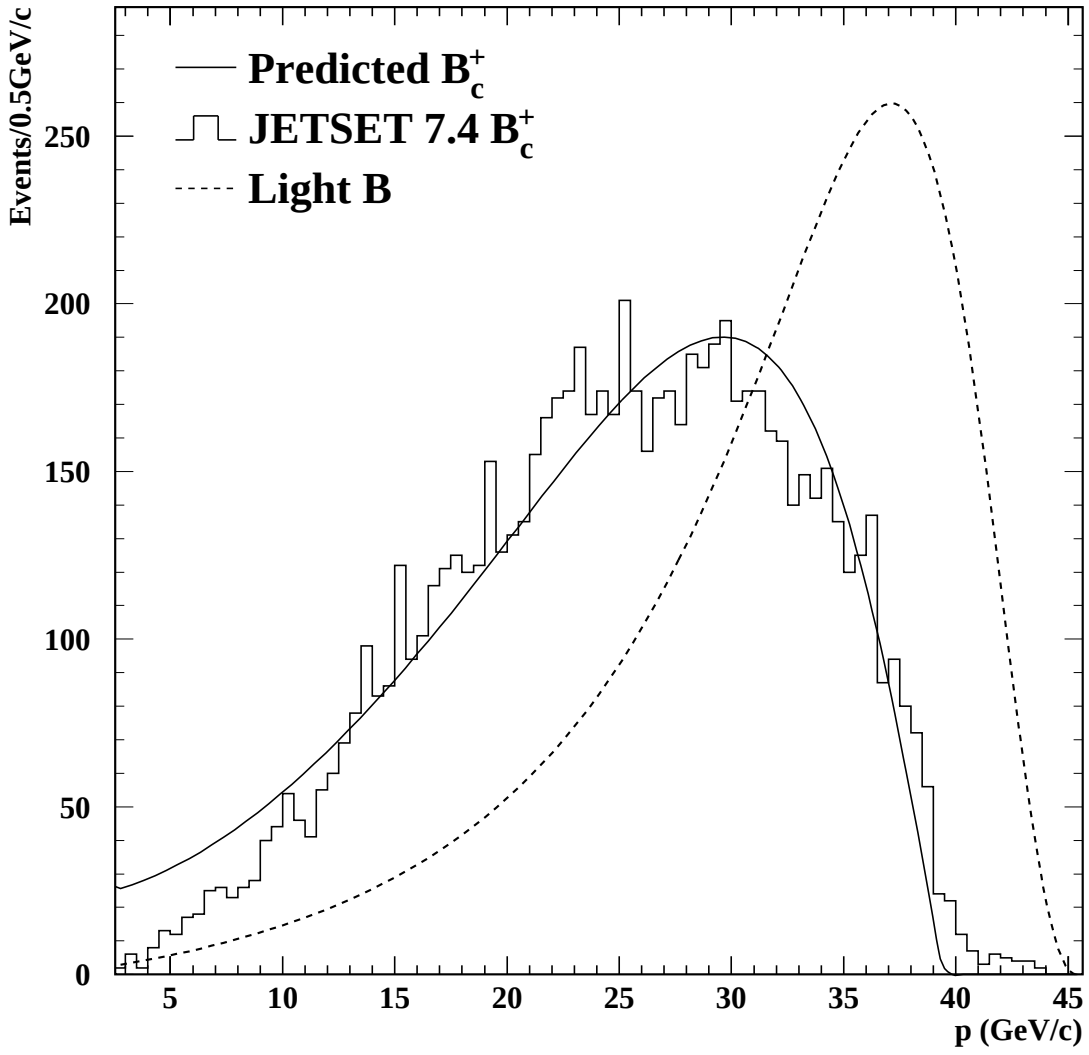

Figure 2: Momentum spectrum of B_c mesons from the process $Z^0 \to b\bar{b} \to B_c X$ generated using JETSET 7.4 (histogram). Overlaid is the prediction of the theoretical model in reference [2] (solid line). Also shown is the momentum distribution of light B mesons for the OPAL tune of JETSET 7.4 in which the mean energy of b hadrons agrees with the experimental value (dashed line).

candidates combined to form J/ψ candidates in the $B_c^+ \to J/\psi \ell^+ \nu$ mode must satisfy the criteria of the "strong" muon identification. J/ψ candidates are required to have an invariant mass within the range 2.9 to 3.3 GeV/c^2 for the $\mu^+\mu^-$ channel, and within the range 2.8 to 3.3 GeV/c^2 for the e^+e^- channel. The $J/\psi \to e^+e^-$ candidate range is extended to lower masses in order to include the tail in the $J/\psi \to e^+e^-$ invariant mass distribution due to electron bremsstrahlung radiation in the detector and J/ψ radiative decays. Figure 3 shows the lepton pair invariant mass distributions for leptons selected with the "normal" lepton selection in the range 2.5 to 3.5 GeV/c^2, where the J/ψ peak is clearly visible in both e^+e^- and $\mu^+\mu^-$ modes. The peak position and width are consistent with the J/ψ mass and the expected resolution of the OPAL detector. We find a total of 354 $J/\psi \to e^+e^-$ candidates and 551 $J/\psi \to \mu^+\mu^-$ candidates using the normal muon selection. We find 391 $J/\psi \to \mu^+\mu^-$ candidates using the "strong" muon selection.

4.2 Selection of B_c Candidates

The dominant background to the sample of B_c candidates is from random combinations of J/ψ's produced in b hadron decays with other tracks from b hadron decays or from fragmentation. Given the fact that at best a few events are expected in each channel, it is crucial that the combinatorial background be reduced to below the level of the expected signals. The selection criteria were developed by studying Monte Carlo simulated events containing the signal processes, and the simulated sample of five-flavor Z^0 events (described above). In general, significant background suppression can be achieved by taking advantage of the hard momentum spectrum and the long lifetime of the b hadrons. However, the soft momentum spectrum of the B_c weakens the discrimination power of any momentum cut. Furthermore, since there is large uncertainty in the predictions of the B_c lifetime, no decay length cut is used. The criteria are summarised below:

a. In all decay modes J/ψ candidates are kinematically constrained to the nominal J/ψ mass in order to improve the B_c mass resolution.

b. For the exclusive modes, $J/\psi\pi^+$ and $J/\psi a_1^+$, we require that the dE/dx measurement for each pion candidate be "consistent" with the expected value for a pion (as described in section 3).

c. In the semileptonic mode, $B_c^+ \to J/\psi \ell^+ \nu$, there is a large background at lower masses involving fake J/ψ or J/ψ combined with fake leptons or leptons from cascade decays. This background is reduced by using the "strong" muon identification for all muon candidates and requiring the ℓ^+ lepton track momentum $p > 4.0$ GeV/c.

d. For $J/\psi\pi^+\pi^-\pi^+$ combinations, we require that the three-pion combination be consistent with resulting from the decay $a_1^+ \to \rho^0\pi^+$, where $\rho^0 \to \pi^+\pi^-$. The invariant mass of the three pion combination must be consistent with the a_1 mass, $(1.0 < M(\pi^+\pi^-\pi^+) < 1.6)$ GeV/c^2, and the invariant mass of at least one of the two $\pi^+\pi^-$ pairs must be in the ρ^0 mass range, $(0.65 < M(\pi^+\pi^-) < 0.90)$ GeV/c^2.

e. All tracks from the B_c must be consistent with originating from the same decay vertex. For each B_c candidate we determine the decay vertex from the intersection of the tracks, including the tracks forming the J/ψ candidate, in the x-y plane. We require the χ^2 probability of the vertex fit to exceed 1%.

f. Since the combinatorial backgrounds are largest at low momenta, we impose a minimum momentum cut on the B_c candidates. For the $J/\psi\ell^+\nu$ mode, where the full momentum of the candidate is not reconstructed, we require the momentum of the $J/\psi\ell^+$ combination to exceed 30% of the beam energy. For $J/\psi\pi^+$ combinations we require the momentum of the B_c candidate to exceed 55% of the beam energy. For the $B_c^+ \to J/\psi a_1^+$ candidates, where the combinatorial background is more severe, the candidate momentum is required to exceed 70% of the beam energy.

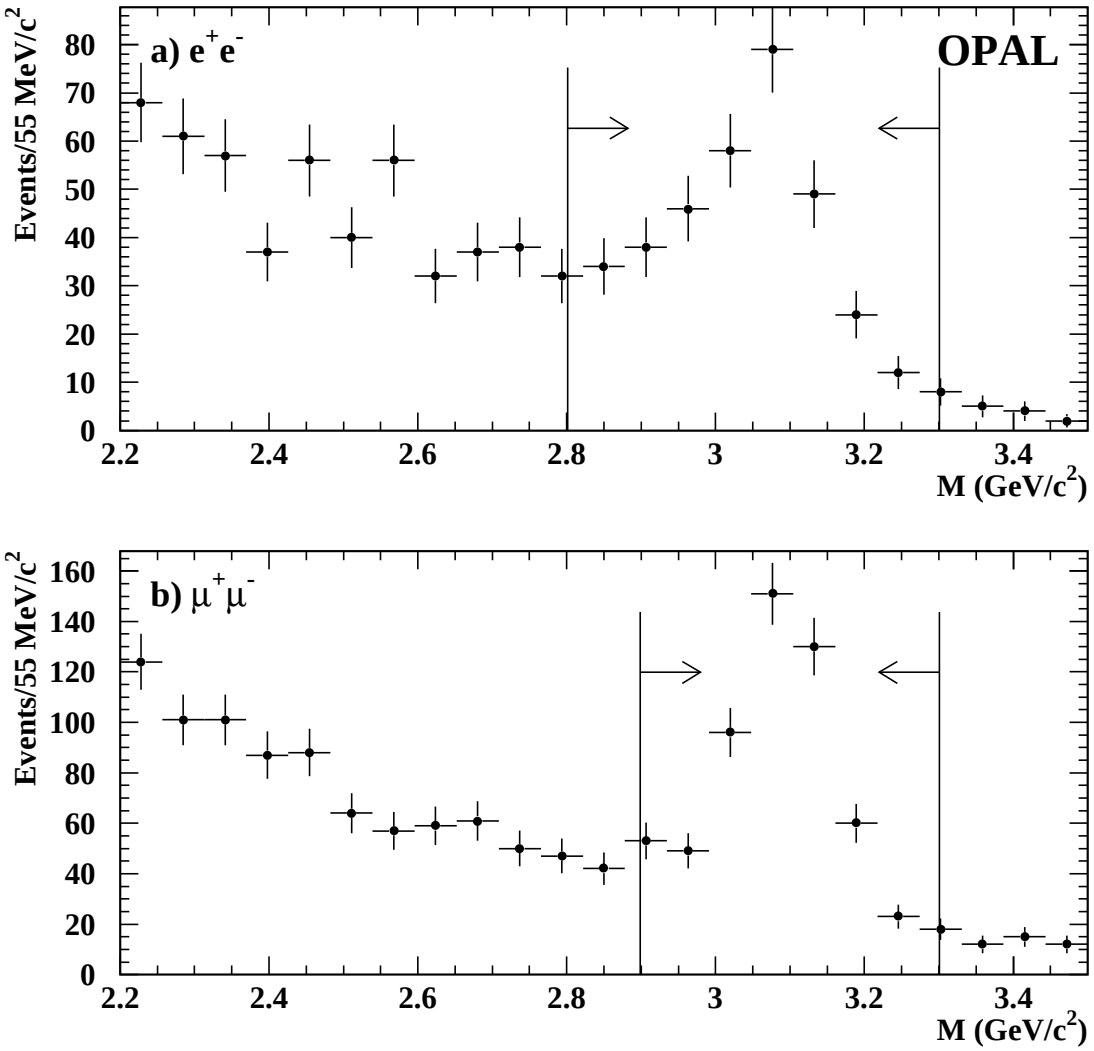

Figure 3: Invariant mass spectrum of selected (a) e^+e^-, and (b) $\mu^+\mu^-$ pairs. Also shown are the mass regions where the J/ψ candidates are defined.

g. For the exclusive modes, we take advantage of the fact that the decay products of a pseudoscalar meson are isotropically distributed in its rest frame. We define θ^* as the angle between the B_c candidate direction and the direction of the J/ψ in the B_c rest frame. Since the combinatorial background mainly peaks near the backward direction ($\cos\theta^* = -1.0$), we require $\cos\theta^* > -0.8$.

h. For the exclusive modes, the invariant mass of the B_c candidates must be in the mass interval 6.0 to 6.5 GeV/c^2 (hereafter referred to as the signal region) which is centered around the predicted B_c mass, with a width which is about three times the B_c mass resolution ($\simeq$ 80 MeV/c^2) on each side. The mass window includes the entire range of predictions for the B_c mass. For the semileptonic mode, where the full invariant mass cannot be calculated, the invariant mass of the $J/\psi\ell^+$ combination is used to define the signal region. The rarity of random combinations of three leptons in hadronic Z^0 decays combined with the high mass of the B_c produces a natural separation point between the signal and the background combinations. Figure 4 shows the invariant mass distribution for $J/\psi\ell^+$ combinations from a sample of simulated $B_c^+ \to J/\psi\ell^+\nu$ decays, along with the distribution of the combinatorial background from simulated samples of the $B \to J/\psi X$ and prompt J/ψ events (see the following section for detail). The signal distribution peaks above 4.0 GeV/c^2 and the background combinations are mostly at lower masses. Hence we restrict the signal region to the mass interval 4.0 to 6.5 GeV/c^2.

i. $B^+ \to J/\psi K^+$ decays can fake $B_c^+ \to J/\psi\ell^+\nu$ decays if the kaon is misidentified as a lepton. For the semileptonic mode we reject candidates that have a reconstructed mass within 3σ in mass resolution ($\sigma \simeq$ 60 MeV/c^2) of the measured B^+ mass when the third lepton candidate is assigned the kaon mass.

4.3 Estimation of Reconstruction Efficiencies and the Background Levels

The reconstruction efficiencies are calculated from Monte Carlo generated event samples, with the B_c meson simulated at a mass of 6.25 GeV/c^2. In the $J/\psi\pi^+$ mode the leptons from the J/ψ decay are expected to have a $\sin^2\theta$ angular distribution with respect to the J/ψ direction in the B_c rest-frame. In order to simulate this distribution, which was not included in the Monte Carlo generator, the selected events in the $J/\psi\pi^+$ mode were reweighted. For the decay $B_c^+ \to J/\psi a_1^+$ we conservatively assume an a_1^+ width of 400 MeV. Each sample is composed of events with the appropriate B_c decay and subsequent $J/\psi \to \ell^+\ell^-$ decay. The mass resolution is found to be about 80 MeV/c^2 in the modes $J/\psi\pi^+$ and $J/\psi a_1^+$. The reconstruction efficiencies for these modes are (10.0 $\pm$ 0.7)% and (1.8 $\pm$ 0.3)%, respectively, and (5.5 $\pm$ 0.5)% for the semileptonic mode $B_c^+ \to J/\psi\ell^+\nu$, where the errors are due to Monte Carlo statistics. The reconstruction efficiency is sensitive to the B_c momentum distribution. An estimate of this sensitivity is found by comparing the efficiencies obtained using the distribution predicted by JETSET 7.4 with those obtained assuming the theoretical calculations of reference [2]. Values of $m_b = (4.9 \pm 0.2)$ GeV/c^2 and $m_c = (1.5 \pm 0.2)$ GeV/c^2 were used for the input quark masses [3]. In the $J/\psi\pi^+$ mode the difference is 16.3%. For the $J/\psi a_1^+$ mode, where a harder cut of $x_E > 0.7$ is applied, a difference of 37.9% is found. In the semileptonic mode the difference is 5.7%. We take the systematic errors on the efficiencies to be one half of the difference for each mode.

The expected background level in each channel is determined by searching for B_c decays in the simulated hadronic Z^0 event sample. According to Monte Carlo simulations the background combinations at masses below the signal region are dominated by the combinations of a real J/ψ with random tracks from b hadron decays or from the fragmentation processes. The J/ψ mesons originate dominantly from the decays of b hadrons, with a small fraction, (4.8 $\pm$ 1.7 $\pm$ 1.7)% [23], of prompt J/ψ (J/ψ resulting from the fragmentation processes). In total, the simulated hadronic event sample contains 2800 events containing a leptonic J/ψ decay. To improve the statistical significance of the background studies we apply the B_c search to a sample of 80,000 hadronic Z^0 decays containing the process $B \to J/\psi X$,

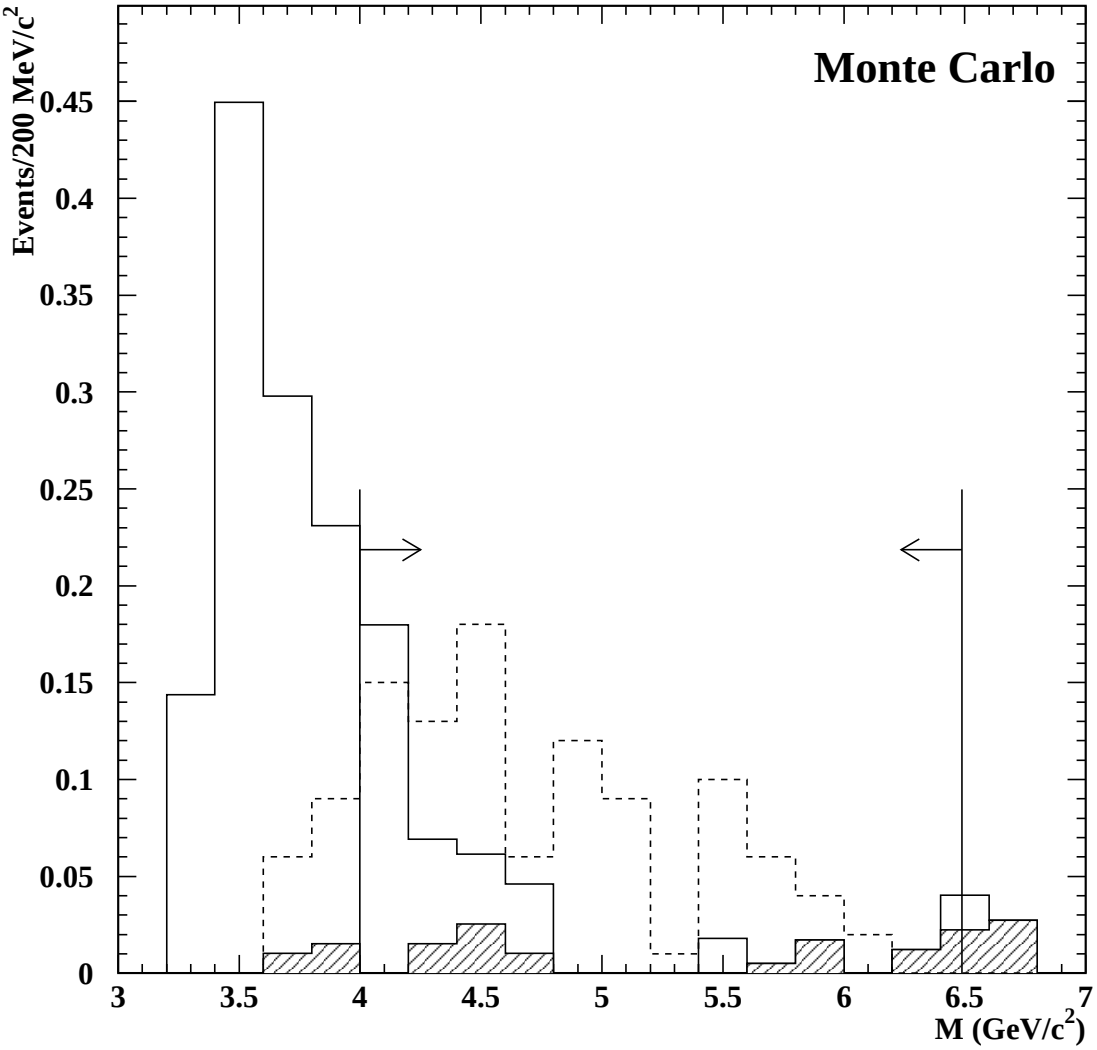

Figure 4: Invariant mass distribution of reconstructed $J/\psi\ell^+$ combinations from a simulated sample of $B_c^+ \to J/\psi\ell^+\nu$ decays (dashed open histogram), and combinatorial background from enriched samples of Monte Carlo simulated $B \to J/\psi X$ (solid open histogram) and prompt J/ψ (hatched histogram) events. The backgrounds are normalised to the number of events expected in the data sample. The normalisation of the signal is arbitrary. Also shown is the mass region where the B_c candidates are defined.

where a $J/\psi \to \ell^+\ell^-$ decay is present in each event. This Monte Carlo sample is equivalent to 30 times the size of the data sample. In addition, the B_c search was applied to two samples of 4000 events containing the processes $Z^0 \to J/\psi q\bar{q}$ and $Z^0 \to J/\psi c\bar{c}$ in order to study background due to prompt J/ψ production from gluon fragmentation and c quark fragmentation, respectively, which are the predicted dominant production mechanisms for prompt J/ψ [24]. The predicted branching ratios for these processes are $Br(Z^0 \to J/\psi q\bar{q}) = 1.9 \times 10^{-4}$ and $Br(Z^0 \to J/\psi c\bar{c}) = 0.8 \times 10^{-4}$. These Monte Carlo sets are equivalent to 40 and 100 times the size of the data sample, respectively.

The resulting invariant mass distributions for the B_c candidates in the three modes are shown in figure 5. From these distributions we estimate the background level (see table 1) by counting the number of candidates in the signal region and normalising to the number of events expected in the data sample. The contribution to the background from $B \to J/\psi X$ events is normalised using the measured rate $Br(Z^0 \to J/\psi X) = (3.9 \pm 0.2 \pm 0.3) \times 10^{-3}$ [5]. The contribution from prompt J/ψ is normalised using the measured rate of prompt J/ψ production $Br(Z^0 \to \text{ prompt } J/\psi X) = (1.9 \pm 0.7 \pm 0.7) \times 10^{-4}$, with the two components of the prompt J/ψ signal each assigned a fraction of the total branching rate according to the ratio of their theoretical production rates. The measured rate of prompt J/ψ production is in agreement with the theoretical rates. The uncertainty in the normalisation factors is used as a systematic error for each background estimate.

Background	Decay Mode		
	$B_c^+ \to J/\psi\pi^+$	$B_c^+ \to J/\psi a_1^+$	$B_c^+ \to J/\psi\ell^+\nu$
$B \to J/\psi X$	$0.22 \pm 0.09 \pm 0.02$	$1.01 \pm 0.19 \pm 0.09$	$0.61 \pm 0.15 \pm 0.06$
J/ψ(c quark frag.)	$0.24 \pm 0.05 \pm 0.13$	$0.07 \pm 0.03 \pm 0.04$	$0.13 \pm 0.04 \pm 0.07$
J/ψ(gluon frag.)	$0.17 \pm 0.06 \pm 0.09$	$0.02 \pm 0.02 \pm 0.01$	$0.07 \pm 0.04 \pm 0.04$
Total	$0.63 \pm 0.12 \pm 0.16$	$1.10 \pm 0.19 \pm 0.10$	$0.82 \pm 0.16 \pm 0.10$

Table 1: Background estimates from samples of 80,000 $B \to J/\psi X$ enriched events, 4000 prompt J/ψ from the gluon fragmentation process, $Z^0 \to J/\psi q\bar{q}$, and 4000 prompt J/ψ from the c quark fragmentation process, $Z^0 \to J/\psi c\bar{c}$. The first error is statistical and the second is systematic.

5 Results and Upper Bounds on the Production Rates

Figure 6 shows the invariant mass distributions of the $J/\psi\pi^+$, $J/\psi a_1^+$, and $J/\psi\ell^+\nu$ candidates in the data sample. The shapes and overall levels of the distributions below the signal regions are consistent with the distributions obtained from the simulated background samples. In the mode $J/\psi\pi^+$ we find two events in the signal range 6.0 to 6.5 GeV/c^2. The invariant masses of the two B_c candidates are (6.29 ± 0.17) GeV/c^2 and (6.33 ± 0.063) GeV/c^2. The errors are calculated from the errors on the track parameters. The reconstructed decay times of the two candidates are $\tau = (-0.06 \pm 0.19)$ ps and $\tau = (0.09 \pm 0.10)$ ps, respectively. The estimated background in this mode is (0.63 ± 0.20) events. The probability for a background of 0.63 events to fluctuate to 2 or more is 13.2%. In the mode $J/\psi\ell^+\nu$ we find one event in the signal region. The mass of the candidate $J/\psi\ell^+$ combination is 5.76 GeV/c^2. The momentum is 15.4 GeV/c. The reconstructed decay length is (0.14 ± 0.14) cm. The estimated background in this mode is (0.82 ± 0.19) events. In the signal region above the mass of the candidate event, 5.76 to 6.5 GeV/c^2, the probability to observe one or more events from background is 8.9%, while the efficiency is reduced to (0.6 ± 0.2)%. There are no candidate events in the $J/\psi a_1^+$ mode in the signal region compared with an estimated background of (1.10 ± 0.22) events.

We determine an upper bound at 90% confidence level on the number of events in each channel by applying Poisson statistics to the number of events observed in the signal region, without background subtraction. This is used to calculate an upper limit on the production rate from:

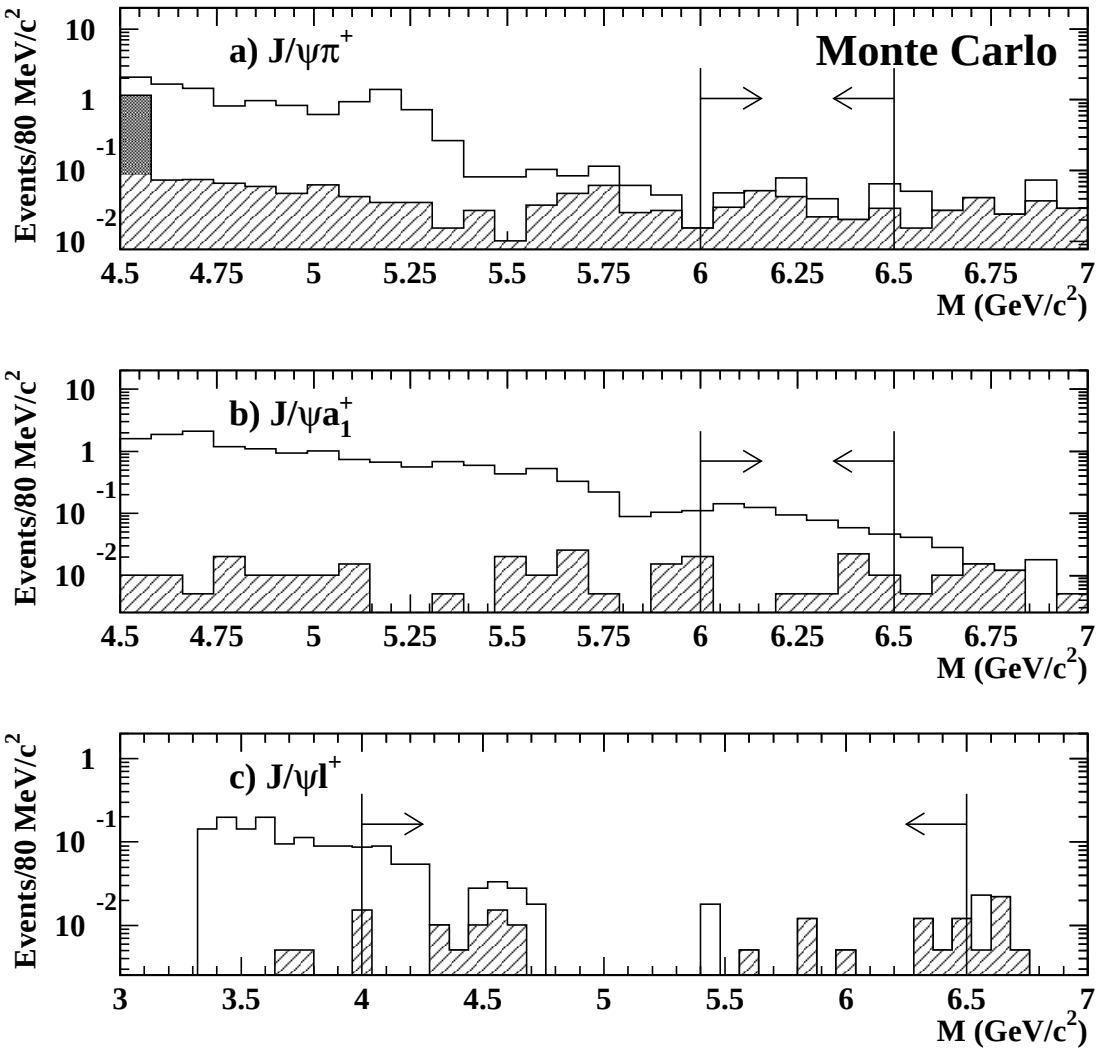

Figure 5: Invariant mass distribution of (a) $J/\psi\pi^+$ combinations, (b) $J/\psi a_1^+$ combinations and (c) $J/\psi\ell^+$ combinations in the simulated background samples. Background events from the process $B \to J/\psi X$ are represented by the open histogram. Background events from prompt J/ψ processes are represented by the hatched histogram. Background events involving fake J/ψ are represented by the shaded histogram. Also shown are the mass regions where the B_c candidates are defined.

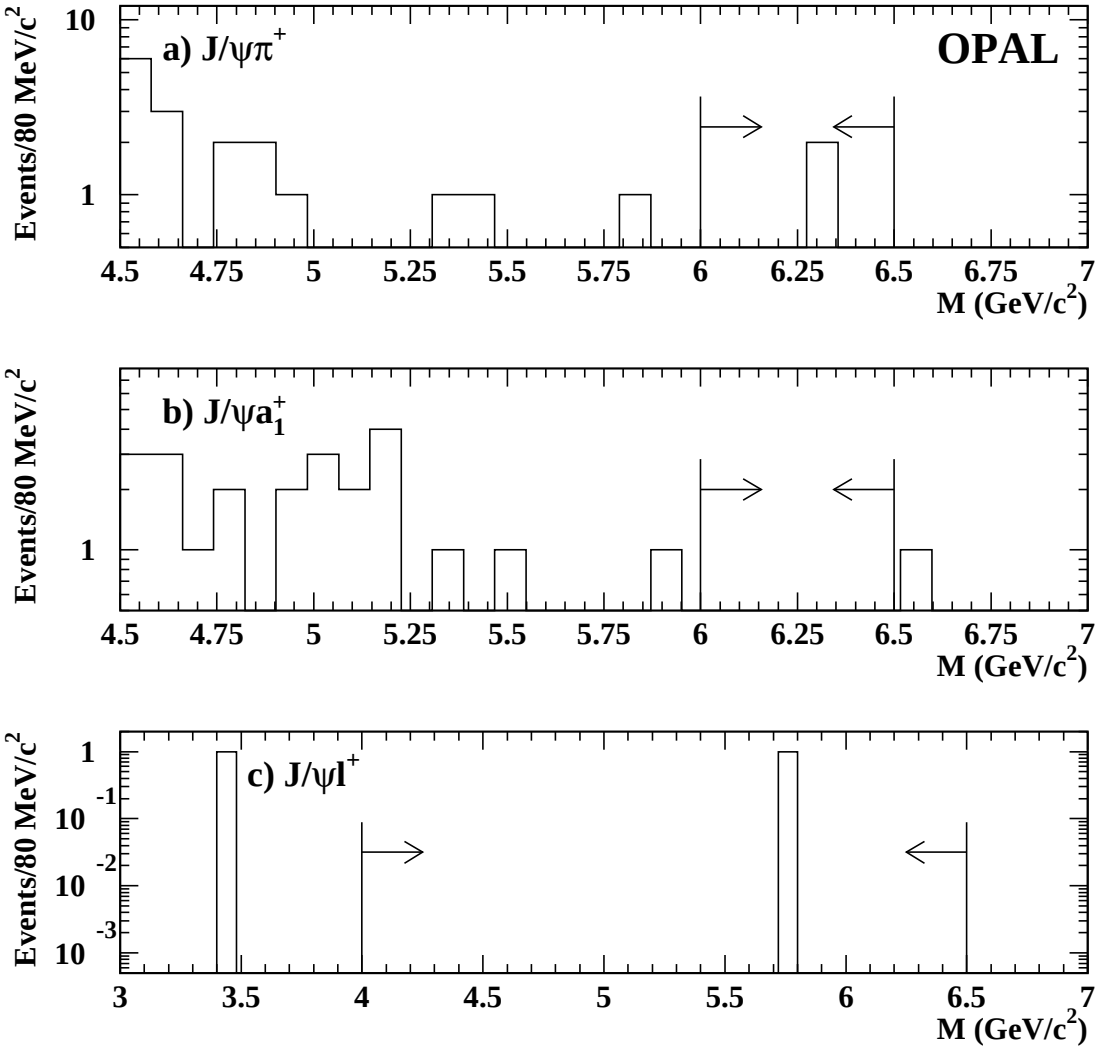

Figure 6: Invariant mass distribution of (a) $J/\psi\pi^+$ combinations, (b) $J/\psi a_1^+$ combinations and (c) $J/\psi\ell^+$ combinations in the data sample. Also shown are the mass regions where the B_c candidates are defined.

Error Source	Decay Mode		
	$B_c^+ \to J/\psi\pi^+$	$B_c^+ \to J/\psi a_1^+$	$B_c^+ \to J/\psi\ell^+\nu$
MC statistics	7.2%	16.6%	9.1%
B_c fragmentation	8.2%	19.0%	2.9%
Lepton eff.	6.5%	6.5%	7.5%
Br(J/ψ)	2.3%	2.3%	2.3%
hadronic eff.	0.5%	0.5%	0.5%
final state radiation	0.6%	0.6%	0.6%
Total error	12.8%	26.2%	12.4%

Table 2: Summary of systematic errors on the product branching ratio upper limits.

$$\frac{\mathrm{Br}(Z^0 \to B_c^+ X)}{\mathrm{Br}(Z^0 \to q\bar{q})} \times \mathrm{Br}(B_c^+ \to \text{final state}) = N(\text{at } 90\% \text{ C.L.}) \times \frac{\epsilon_{\mathrm{had}}}{(N(Z^0) \times \epsilon \times \mathrm{Br}(J/\psi \to \ell^+\ell^-))},$$

where $N(Z^0)$ is the total number of hadronic Z^0 events in the data sample; ϵ_{had} is the hadronic event selection efficiency, 0.981 ± 0.005; ϵ is the reconstruction efficiency for each mode; and Br($J/\psi \to \ell^+\ell^-$) is the branching ratio for the leptonic decays of J/ψ, $J/\psi \to e^+e^-$ and $J/\psi \to \mu^+\mu^-$, 0.1203 ± 0.0028 [25]. For the mode $B_c^+ \to J/\psi a_1^+$, we also account for the branching ratio $\mathrm{Br}(a_1^+ \to \rho^0\pi^+) = 0.5$. The total systematic uncertainties on the branching ratio upper limits for each mode are shown in table 2. These systematic uncertainties are included in the following 90% confidence level upper limits using the technique of ref. [26]:

$$\frac{\mathrm{Br}(Z^0 \to B_c^+ X)}{\mathrm{Br}(Z^0 \to q\bar{q})} \times \mathrm{Br}(B_c^+ \to J/\psi\pi^+) < 1.06 \times 10^{-4},$$

$$\frac{\mathrm{Br}(Z^0 \to B_c^+ X)}{\mathrm{Br}(Z^0 \to q\bar{q})} \times \mathrm{Br}(B_c^+ \to J/\psi a_1^+) < 5.29 \times 10^{-4},$$

$$\frac{\mathrm{Br}(Z^0 \to B_c^+ X)}{\mathrm{Br}(Z^0 \to q\bar{q})} \times \mathrm{Br}(B_c^+ \to J/\psi\ell^+\nu) < 6.96 \times 10^{-5},$$

where the branching ratio for the mode $B_c^+ \to J/\psi\ell^+\nu$ is for decay to either $J/\psi\ e^+\nu$ or $J/\psi\mu^+\nu$.

If we interpret the two candidate events in the $B_c^+ \to J/\psi\pi^+$ mode as signal we find a branching ratio of,

$$\frac{\mathrm{Br}(Z^0 \to B_c^+ X)}{\mathrm{Br}(Z^0 \to q\bar{q})} \times \mathrm{Br}(B_c^+ \to J/\psi\pi^+) = (3.8^{+5.0}_{-2.4} \pm 0.5) \times 10^{-5},$$

where the first error is statistical and the second systematic.

6 Conclusion

We have performed a search for B_c meson decays in data collected with the OPAL detector at LEP. Two candidate $B_c \to J/\psi\pi^+$ decays are observed in a mass window around the theoretical prediction of the B_c mass, compared with an estimated background of (0.63 ± 0.20) events in this mode. The weighted average mass of the two candidates is (6.32 ± 0.06) GeV/c^2, which is consistent with the predicted mass of the B_c meson. One candidate is observed in the mode $B_c^+ \to J/\psi\ell^+\nu$, with a $J/\psi\ell^+$ mass of 5.76 GeV/c^2. The estimated background in this mode is (0.82 ± 0.19) events. We have also searched for the decay $B_c^+ \to J/\psi a_1^+$, but no candidate events were observed. The estimated background in this mode is (1.10 ± 0.22) events. Upper limits at the 90% confidence level are calculated for the production rates of these processes,

$$\frac{\mathrm{Br}(Z^0 \to B_c^+ X)}{\mathrm{Br}(Z^0 \to q\bar{q})} \times \mathrm{Br}(B_c^+ \to J/\psi\pi^+) < 1.06 \times 10^{-4},$$

$$\frac{\mathrm{Br}(Z^0 \to B_c^+ X)}{\mathrm{Br}(Z^0 \to q\bar{q})} \times \mathrm{Br}(B_c^+ \to J/\psi a_1^+) < 5.29 \times 10^{-4},$$

$$\frac{\mathrm{Br}(Z^0 \to B_c^+ X)}{\mathrm{Br}(Z^0 \to q\bar{q})} \times \mathrm{Br}(B_c^+ \to J/\psi\ell^+\nu) < 6.96 \times 10^{-5}.$$

The branching ratio limits for the $B_c^+ \to J/\psi\pi^+$ and $B_c^+ \to J/\psi\ell^+\nu$ mode are comparable with the limits reported by the ALEPH, DELPHI and CDF collaborations [27][28][29].

7 Acknowledgements

We particularly wish to thank the SL Division for the efficient operation of the LEP accelerator at all energies and for their continuing close cooperation with our experimental group. We thank our colleagues from CEA, DAPNIA/SPP, CE-Saclay for their efforts over the years on the time-of-flight and trigger systems which we continue to use. In addition to the support staff at our own institutions we are pleased to acknowledge the
Department of Energy, USA,
National Science Foundation, USA,
Particle Physics and Astronomy Research Council, UK,
Natural Sciences and Engineering Research Council, Canada,
Israel Science Foundation, administered by the Israel Academy of Science and Humanities,
Minerva Gesellschaft,
Benoziyo Center for High Energy Physics,
Japanese Ministry of Education, Science and Culture (the Monbusho) and a grant under the Monbusho International Science Research Program,
German Israeli Bi-national Science Foundation (GIF),
Bundesministerium für Bildung, Wissenschaft, Forschung und Technologie, Germany,
National Research Council of Canada,
Research Corporation, USA,
Hungarian Foundation for Scientific Research, OTKA T-016660, T023793 and OTKA F-023259.

References

[1] E. J. Eichten and C. Quigg, Phys. Rev. **D49** (1994) 5845;
S. S. Gershtein, V. V. Kiselev, A. K. Likhoded, and A. V. Tkabladze, Phys. Rev. **D51** (1995) 3613.

[2] Chao-Hsi Chang and Yu-Qi Chen, Phys. Rev. **D46** (1992) 3845.

[3] E. Braaten and K. Cheung, Phys. Rev. **D48** (1993) 5049.

[4] S. S. Gershtein, A. K. Likhoded, and S. R. Slabospitsky, Int. J. Mod. Phys. **6** (1991) 2309.

[5] OPAL Collab., G. Alexander et al., Z. Phys. **C70** (1996) 197.

[6] OPAL Collaboration, K. Ahmet et al., Nucl. Instrum. and Meth. **A305** (1991) 275.

[7] P. P. Allport et al., Nucl. Instrum. and Meth. **A324** (1993) 34;
P. P. Allport et al., Nucl. Instrum. and Meth. **A346** (1994) 476.

[8] M. Hauschild et al., Nucl. Instrum. and Meth. **A314** (1992) 74.

[9] OPAL Collab., G. Alexander et al., Z. Phys. **C52** (1991) 175.

[10] OPAL Collab., G. Alexander et al., Z. Phys. **C70** (1996) 357.

[11] OPAL Collab., K. Ackerstaff et al., Z. Phys. **C74** (1997) 423.

[12] OPAL Collab., R. Akers et al., Z. Phys. **C60** (1993) 199.

[13] OPAL Collab., P. Acton et al., Z. Phys. **C58** (1993) 523.

[14] OPAL Collab., P. Acton et al., Z. Phys. **C63** (1994) 197.

[15] T. Sjöstrand, Comp.Phys.Comm. **39** (1986) 347;
M. Bengtsson and T. Sjöstrand, Comp. Phys. Comm. **43** (1987) 367;
M. Bengtsson and T. Sjöstrand, Nucl. Phys. **B289** (1987) 810;
T. Sjöstrand, CERN-TH/6488-92.

[16] C. Peterson, D. Schlatter, I. Schmitt and P. Zerwas, Phys. Rev. **D27** (1983) 105.

[17] OPAL Collab., G. Alexander et al., Phys. Lett. **B364** (1995) 93.

[18] Parameter values of JETSET were tuned to describe global event shape variables: OPAL Collab.
R. Akers et al., Z. Phys. **C65** (1995) 31.

[19] L. Montanet et al., Phys. Rev. **D50** (1994) 1.

[20] J. Allison et al., Nucl. Instrum. and Meth. **A317** (1992) 47.

[21] F. A. Berends and R Kleiss, Nucl. Phys. **B177** (1981) 237.

[22] O. Nicrosini and L. Trentadue, Phys. Lett. **B196** (1987) 551;
J. P. Alexander et al., Phys. Rev. **D37** (1988) 56.

[23] OPAL Collab., G. Alexander et al., Phys. Lett. **B384** (1996) 343.

[24] P. Cho, Phys. Lett. **B368** (1996) 171;
P. Cho and A. Leibovich, Phys. Rev. **D53** (1996) 150.

[25] R. M. Barnett et al., Phys. Rev. **D54** (1996) 1.

[26] R. D. Cousins and V. L. Highland, Nucl. Instrum. and Meth. **A320** (1992) 331.

[27] ALEPH Collaboration, D. Abbaneo et al., CERN-PPE/97-026, submitted to Phys. Lett. **B**.

[28] DELPHI Collaboration, P. Abreu et al., CERN-PPE/96-194, submitted to Phys. Lett. **B**.

[29] CDF Collaboration, F. Abe et al., Phys. Rev. Lett. **77** (1996) 5176.